# Development, Validation and Application of an ANN-based Large Eddy Simulation Subgrid-Scale Turbulence model for dense gas flows

Alexis Giauque, Aurélien Vadrot, Christophe Corre

▶ **To cite this version:**

Alexis Giauque, Aurélien Vadrot, Christophe Corre. Development, Validation and Application of an ANN-based Large Eddy Simulation Subgrid-Scale Turbulence model for dense gas flows. 4th International Seminar on Non-Ideal Compressible Fluid Dynamics for Propulsion and Power. NICFD 2022, Nov 2022, London, United Kingdom. pp.43-52, 10.1007/978-3-031-30936-6_5 . hal-04928384

**HAL Id: hal-04928384**
**https://hal.science/hal-04928384v1**

Submitted on 4 Feb 2025

**HAL** is a multi-disciplinary open access archive for the deposit and dissemination of scientific research documents, whether they are published or not. The documents may come from teaching and research institutions in France or abroad, or from public or private research centers.

L'archive ouverte pluridisciplinaire **HAL**, est destinée au dépôt et à la diffusion de documents scientifiques de niveau recherche, publiés ou non, émanant des établissements d'enseignement et de recherche français ou étrangers, des laboratoires publics ou privés.

NICFD 2022
For Propulsion & Power

# Development, Validation and Application of an ANN-based Large Eddy Simulation Subgrid-Scale Turbulence model for dense gas flows

**Alexis Giauque**
**Univ Lyon,**
**Ecole Centrale de Lyon,**
**Univ Claude Bernard Lyon 1,**
**INSA Lyon,**
**LMFA, UMR 5509,**
alexis.giauque@ec-lyon.fr
Ecully, 69130, AURA, France

**Aurélien Vadrot**
**Univ Lyon,**
**Ecole Centrale de Lyon,**
**Univ Claude Bernard Lyon 1,**
**INSA Lyon,**
**LMFA, UMR 5509**
aurelien.vadrot@ec-lyon.fr
Ecully, 69130, AURA, France

**Christophe Corre**
**Univ Lyon,**
**Ecole Centrale de Lyon,**
**Univ Claude Bernard Lyon 1,**
**INSA Lyon,**
**LMFA, UMR 5509**
christophe.corre@ec-lyon.fr
Ecully, 69130, AURA, France

## ABSTRACT

Using a DNS database (available to the NICFD research community) including homogeneous isotropic turbulence (HIT), mixing layers and channel flows, the authors have developed a novel LES model for the Subgrid-Scale (SGS) turbulent Reynolds tensor based on artificial neural networks (ANN) with optimized hyperparameters. Particular attention has been paid to ensure Galilean invariance properties are satisfied by the ANN-based model. To accommodate the large size of the database (over 500 million samples), the ANN is trained on a parallel CPU architecture. *A priori* performance reveals determination coefficients ($r^2$-score) larger than 0.9 can be achieved, yielding an accurate prediction of the SGS turbulent Reynolds tensor magnitude for flow conditions never met during training. *A posteriori* validation is performed by implementing the model into AVBP, a LES solver developed at CERFACS [10]. The computation of a dense gas mixing layer at a convective Mach number of 2.2 shows that the newly developed ANN-based model provides levels of accuracy comparable with or even better than those provided by existing models (Implicit LES, Sigma model [13]). To further assess the ANN-based model, a 3D ORC turbine configuration is computed and the numerical prediction is compared with measurements gathered by Baumgartner, Otter and Wheeler [1] at Cambridge University and presented at NICFD 2020. Preliminary results from this recently launched European PRACE project are presented.
*Keywords: ORC, Large Eddy Simulation, SGS Modeling, Dense gas, Machine Learning*

## 1 INTRODUCTION

Global warming due to the release of huge amounts of $CO_2$ in the atmosphere generated by the consumption of fossil fuel is now considered as one of the most important threat to the stability of modern society. To reduce the production of $CO_2$, renewable energies are currently being developed at an accelerated pace. Among the possible technological solutions available, the Organic Rankine Cycle has been proposed to harvest low to moderate temperature heat sources. ORC systems use, instead of water, organic fluids displaying low boiling temperatures and large heat capacities. Among those fluids, some, when in their gaseous form and in specific thermodynamic conditions, are called dense gases. Dense gases are characterized by a fundamental derivative $\Gamma$ lower than unity. Following this definition, the speed of sound in these gases decreases with increasing density along isentropic lines. Numerous phenomena occur in flows of dense gases that are related to their specific thermodynamic nature: lower speeds of sound are reached and most importantly the strength of shockwaves is significantly reduced. This phenomenon, first evidenced numerically by Schnerr and Leidner in 1996 [17] and again shown by Cinnella and Congedo in 2005 [2], is at the origin of a renewed interest for dense gases in the context of ORC. In 2016, Dura Galiana et al. [4, 5] show that up to $2/3$ of the losses in turbine expanders comes from viscous effects in the wake. The trailing edge region where the wake starts is both the region of origin of shockwaves necessary for the flow to adapt to the back pressure, and a region displaying a large turbulence activity because of the merging boundary layers coming from the blade. A natural question in this context is that of the interaction between turbulence and thermodynamics in dense gas flows (more specifically in turbine expanders) and its impact on SGS turbulence modeling.

To the best of the authors' knowledge, this question has not yet been addressed and state of the art comparisons between CFD and experiments either rely on Euler equations with a focus on compressibility-induced features [9] or on Large Eddy simulations (LES) using existing subgrid scales models developed in the context of perfect gas flows [11]. To better understand the behavior of turbulence in dense gas flows, the authors have analyzed Direct Numerical Simulations (DNS) in academic configurations such as Homogeneous Isotropic Turbulence, Mixing Layer and Channel Flow. Numerous physical phenomena specific to the dense nature of the gas have been described such as the strongly modified statistics of shocklets in compressible turbulence, the decoupling of internal and kinetic energy in the mixing layer which has also been observed in the channel flow and confirms independent findings from [18]. Among all results, the most striking one, observed by Vadrot during his PhD [19] is the strongly modified growth rate (multiplied by a factor 2) of the dense gas mixing layer when compared to the perfect gas one.

The precise description of losses occurring in ORC turbines requires LES as a way to accurately capture turbulence in general and more specifically features such as boundary layer transition, shockwave/boundary layer interaction and wake turbulence dynamics. LES is now a proven approach in the understanding and fine tuning of complex systems in presence of turbulent phenomena. In this

approach, the most energetic part of the turbulent spectrum is captured by the numerical solver and the remaining part has to be modeled using so called "subgrid" models. Most models have been developed in the context of perfect gases and almost entirely focus on the SubGrid-Scale Reynolds Stress Tensor (SGS RST).
Recent findings by the authors [8] show that (1) additional subgrid-scale terms should be considered in dense gases, (2) usual closure models for the SGS RST lack precision when applied to turbulent dense gas flows. Developing turbulence models for dense gas flows requires to take into account highly non-linear Equations of State (EoS) needed to accurately describe the dense gas thermodynamic behavior. This significantly complexifies the usual modeling strategies and leads the authors to propose instead the use of Artificial Neural Networks (ANN), since they are well adapted to the identification of correlations in a non-linear context. This paper presents the development, validation and application of an ANN-based Large Eddy Simulation Subgrid-Scale Turbulence model for dense gas flows. In Section 2, the methodology used for the development of the model is presented, with a focus on the Galilean invariance of the training data and on the optimization of hyperparameters of the neural network. In section 3, a preliminary *a posteriori* validation of the model is presented to demonstrate the influence of the ANN-based model on (i) the growth rate of a dense gas supersonic mixing layer and (ii) the total pressure distributions experimentally measured in an annular stator configuration at Cambridge University.

## 2 METHODOLOGY : Development of an ANN model for the subgrid-scale Reynolds Tensor in LES

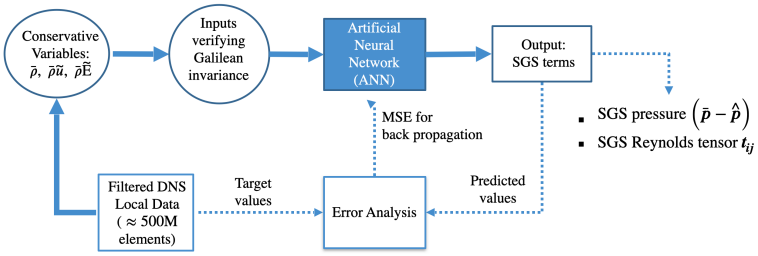


Figure 1: *Schematic representation of the ANN training process*

The general description of the ANN training process is illustrated in Figure 1. Starting from a DNS database of dense gas flows, local data are spatially filtered at a wavelength lying within the inertial range of turbulence for each case considered. In practice, a Gaussian filter is applied with a characteristic wavelength equal to roughly twenty times the initial DNS resolution. These filtered data are composed of all conservative ($\bar{\rho}$, $\bar{\rho}\tilde{u}_i$, $\bar{\rho}\tilde{E}$) and thermodynamic fields ($\hat{p}$,$\hat{T}$) along with their gradients ($\tilde{g}_{ij} = \frac{\partial \tilde{u}_i}{\partial u_j}$,$\vec{\nabla}\hat{p}$,$\vec{\nabla}\hat{T}$). $\bar{\phi}$ denotes the resolved large-scale component of a flow variable ($\phi$). $\tilde{\phi} = \frac{\overline{\rho\phi}}{\bar{\rho}}$ denotes the Favre averaged of a flow variable $\phi$ while $\hat{\phi}$ denotes computable variables that are computed from conservative filtered fields (see [8] for a more detailed description). Components of the Turbulent Reynolds Tensor ($t_{ij} = \bar{\rho}(\widetilde{u_i u_j} - \tilde{u}_i\tilde{u}_j)$) are also stored for later use during training.
Among all the potentially available data when running a LES, actual input data are selected using a sensitivity analysis later described in this paper and preprocessed to satisfy Galilean invariance principles. Following usual practice, the database is then split into a training and a testing part. The training section of the database is used first to fit the parameters of the ANN (*i.e.* the weights and biases of each connection and neuron). The testing section is used next to assess the performance of the ANN and verify the absence of overfitting. To perform this analysis, the ANN prediction is compared to the Reynolds Tensor components target values available in the database.

### 2.1 Description of the database

The methodology used in this study to develop a SGS model tailored for dense gas flows relies on Direct Numerical Simulations (DNS) computed by the authors in the course of the last five years. Figure **??** illustrates the academic dense gas flow configurations considered in this research project: Forced Homogeneous Isotropic Turbulence (Forced-HIT), Channel Flow and Mixing Layer. The reader interested in the details of the comparison of these flows with their perfect gas counterparts is referred to [6, 7] for the Forced-HIT, [8] for the channel and [20, 21] for the mixing layer. The code AVBP, developed at CERFACS, has been used for the development of the database and is also the code used to assess a-posteriori the properties of the developed SGS model. During the course of this entire study, the 3rd order in space and time convective scheme TTGC is used [3].

### 2.2 Choice of the input variables

The choice has been made from the start to consider as input variables only local data taken at the same location where the ANN is expected to predict the Reynolds Tensor components. This choice has been guided by CPU cost considerations in the context of High Performance Computing of dense gas flows. Indeed, other types of non-local neural networks exist such as Convolutional Neural

Networks (non local in space) [16] or networks using LSTM neurons (non local in time). These attractive types of neurons and neural networks are however such that their cost for LES modeling over large discretization grids would eventually prevent their practical use. Using therefore Gaussian-filtered local data only, the additional underlying principle guiding the choice of the ANN input variables is the Galilean invariance principle. This principle is based on a set of invariance properties including translation and rotation of the reference frame and uniform motion with respect to the reference frame. To make sure the ANN prediction satisfies the Galilean invariance principle, the input data should themselves be unchanged when the frame of reference is translated or when one adds a uniform translation motion to the database. Verifying the invariance with respect to the rotation of the frame of reference is more complex. Indeed, except for the HIT, the DNS constituting the database display the bulk flow direction as preferred direction. In order to verify the rotational invariance, each sample is randomly rotated before it is added to the database, with the distribution of rotation angles around the original $x$, $y$ and $z$ axis as flat as possible and ranging from 0 to $2\pi$.
Actual input data used in this work have been initially chosen among all the data potentially available when running a LES. Based on the *a-priori* performance analysis of the ANN-based SGS model, the following set of 15 inputs has been eventually retained: $y^+$, $\tilde{\rho}$, $\tilde{T}$, $\tilde{g}_{ij} = \frac{\partial \tilde{u}_i}{\partial u_j}$, $\tilde{s}_{ij} = \frac{1}{2}\left(\tilde{g}_{ij} + \tilde{g}_{ji}\right)$. Although strain rate tensor components $\tilde{s}_{ij}$ are strongly correlated with velocity gradients $\tilde{g}_{ij}$ and do not improve the *a-priori* performance, it has been observed that they improve the consistency of *a posteriori* ANN-based SGS model predictions.

### 2.3 Optimization of the hyperparameters

The type of ANN used in this work is a multi-layer perceptron (a fully connected class of feedforward ANN). The hyperparameters of the ANN are of two main types. The first type is constitutive of the ANN in the sense that it also applies when the ANN is later used in *a posteriori* validation. Those type-1 hyperparameters are:

- the number of hidden layers,
- the number of neurons in each hidden layer,
- the activation function of each neuron.

The second type of hyperparameters is intrinsically linked to the training of the ANN. Those type-2 hyperparameters are:

- the size of the batches used to train the ANN,
- the optimization algorithm used for back-propagation,
- the measure used to assess the accuracy of the ANN,
- the regularization parameters ($L_2$ regularization in this work) to balance the amplitude of weights over the whole network and to avoid over-fitting.

The most popular methods used to tune an ANN are hyperparameter searches, which browse the hyperparameters space, testing a large number of hyperparameters combinations, for an optimized amount of computational time, in order to identify the one providing the best accuracy. The fundamental issue with these methods is the lack of information they provide about the sensitivity of the ANN to the choice of its hyperparameters: they are often seen as black-box tools which only yield the most effective ANN, with no information provided about the most influential hyperparameters or the most relevant range for each of them. Even though this information is actually stored in the search results, it is rarely exploited.
In this work, in addition to hyperparameter searches, an Hilbert-Schmidt Independence Criterion (HSIC) analysis is performed following the proposal made in [14]. HSIC evaluates in a first step the probability distribution of hyperparameters among tested combinations of hyperparameters randomly selected by the hyperparameters search method, denoted $P(\text{'hyperparameter'})$. In a second step, HSIC computes the probability distribution for an ANN of being among the best decile networks (the 10% of the best ANN), denoted $P(\text{'hyperparameter'}|Z)$, where $Z$ is a random variable which is equal to one if the ANN is among the best decile. Two types of results are eventually obtained: a classification of hyperparameters by rank of importance (Figure 2a)) and the optimal choice for a given hyperparameter (Figure 2b)). In the given example, HSIC allows to identify the significant influence of the optimization algorithm used for back-propagation and recommends the use of the ADAbelief method for optimal ANN performance.

### 2.4 Analysis of the training process

The training process uses the complete training database, combining HIT, channel and mixing layer data with preprocessing to enforce Galilean invariance, over several epochs to optimize the weights and biases of the ANN until the optimization process converges and the accuracy of the model reaches an asymptotic value. Figure 3 illustrates this process for the three off-diagonal terms of the Turbulent Reynolds tensor ($t_{xy}$, $t_{xz}$ and $t_{yz}$). One observes that for the testing database, values of the $r^2$-score larger than 0.9 are reached after 20 to 30 epochs. To illustrate this level of correlation between the filtered DNS data and the ANN model, Figure 4 shows a side-by-side comparison of $t_{xy}$ for the mixing layer at $M_c = 2.2$ from the filtered DNS (Fig. 4 a)) and the ANN prediction (Fig. 4 b)). $M_c = \frac{\Delta u}{c_1 + c_2}$ is

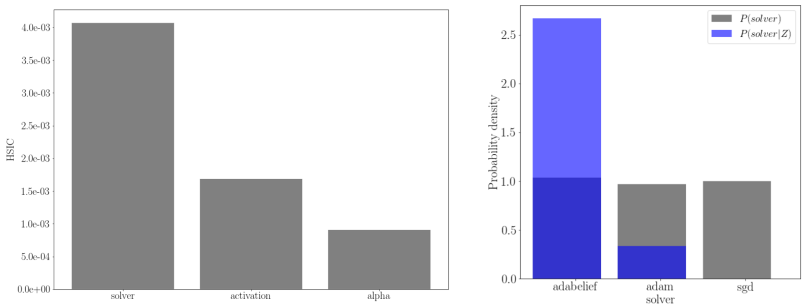


Figure 2: *a) Classification of HSIC and b) Probability density function among solver choices.*

the convective Mach number ($\Delta u$ is the differential speed between upper and lower parts of domain and $c_1$ and $c_2$ are the corresponding sound speeds). Note that the prediction is computed for a temporal solution which was not included in the training database. It can be observed in Figure 4 that the local nature of the ANN model does not preclude the accurate reproduction, both in size and amplitude, of the $t_{xy}$ peak regions.

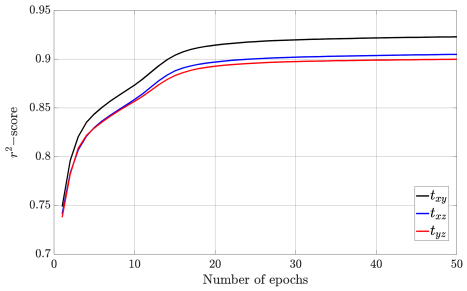


Figure 3: *Evolution of the $r^2-$score computed for the three off-diagonal terms of the Turbulent Reynolds tensor over the testing database as a function of the number of epochs.*

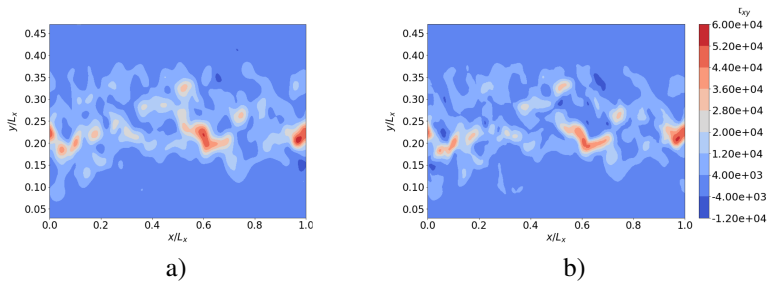


Figure 4: *Comparison of $t_{xy}$ between the (a) true values and (b) the predicted ones.*

## 3 RESULTS : Validation of the ANN-based turbulent closure model

### 3.1 Mixing layer at convective Mach number of 2.2

The ANN model tuned in the previous *a priori* analysis bas been implemented in the LES solver AVBP developed at CERFACS, as an alternative to state-of-the-art SGS models available in this solver. The mixing layer case at $M_c = 2.2$ is considered as a first validation

test-case. Four different meshes are designed to assess the accuracy of the ANN-based model as a function of the grid resolution. For this numerical experiment, the following spatial resolutions are considered : $\Delta/\Delta_{DNS}$ =4, 8, 16 and 32. The first two resolutions are too close to the DNS to be reachable by practical LES. The two coarsest are representative of LES designed to have the turbulent kinetic energy spectrum cut in the inertial regime for large enough Reynolds numbers. Figure 5a) compares the reference DNS temporal evolution of the mixing layer thickness with the LES simulations using the grid $\Delta/\Delta_{DNS} = 32$ and (i) the ANN model, (ii) the Sigma model and (iii) implicit LES. Because of the coarse grid resolution, the initial solution starts for all LES with a mixing layer thickness larger than in the DNS. The evolution of the mixing layer thickness is initially very similar between implicit LES and the ANN model but both strategies start to depart from each other after a non-dimensional time $\tau$ larger than 4000 and eventually the ANN model better recovers the growth rate of the DNS. The Sigma model at first predicts a larger mixing layer but quickly saturates and strongly under-predicts the growth rate later in time. Note that the comparison of the growth rates is meaningful when each computation reaches a linear regime, that is for $\tau \in [6000, 7000]$.
Figure 5b) directly compares the mixing layer growth rates reached in the self-similar regime by each model as a function of the space resolution. It can be seen that for this $M_c = 2.2$ dense gas mixing layer the ANN model consistently better predicts the mixing layer thickness for all four spatial resolutions considered, with an error of 10% maximum with respect to the DNS.

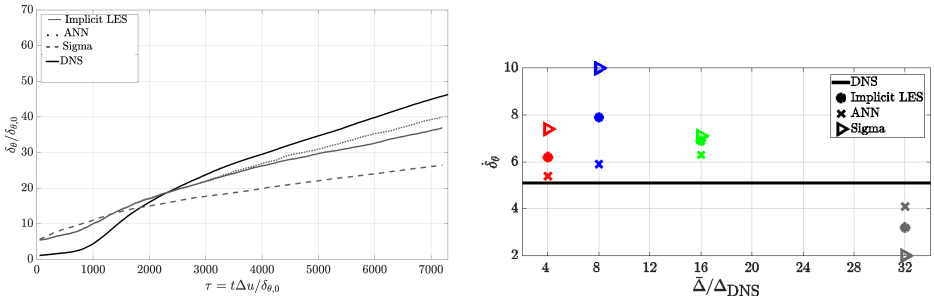


a) b)

Figure 5: *a) Temporal evolution of the momentum thickness for a mixing layer at $M_c = 2.2$. Comparison is made between DNS and three LES at $\Delta/\Delta_{DNS} = 32$. b) Comparison of growth rates for DNS and three LES as a function of the resolution ($\Delta/\Delta_{DNS}$).*

### 3.2 Annular stator case

In order to further assess the accuracy of the ANN-based model for flow configurations representative of industrial applications, it is expected to be applied to the simulation of the annular stator case tested in Cambridge University[1] and presented at the last NICFD conference[15]. More precisely, a comparison is sought between available measurements and LES simulations performed using both the novel model and a state-of-the-art algebraic model (WALE model [12]). Figure 6(a) displays the supersonic annular stator of chord 1cm which leads to Reynolds numbers ($Re = 500000$) that are tractable by LES (see Figure 6(b) for a typical LES flow field visualization). Another interesting feature of this experiment is the relatively large amount of data available thanks to static wall pressure measurements along the shroud and total pressure measurements in the wake. Those can be used to discriminate numerical results obtained through different grid resolutions and turbulence models (see Figure 7). To properly investigate the effect of the ANN model on the LES results, three different grid resolutions are considered: from a coarse grid with 46 million cells and a wall-law to a fine grid with 450 million cells allowing a wall-resolved calculation. Computations are performed on each grid using the classical WALE subgrid scale model or the novel ANN model. Figure 7 presents preliminary results for the total pressure ratio in the wake obtained with the WALE model and compared to experimental measurements. A more detailed comparison will be proposed and discussed at the NICFD 2022 Conference.

## 4 CONCLUSIONS AND FUTURE WORKS

A new modeling strategy has been developed for the SGS turbulent Reynolds tensor using supervised machine learning tools. The optimization and the training of an ANN using a rich database including several dense gas turbulent flow configurations enabled to

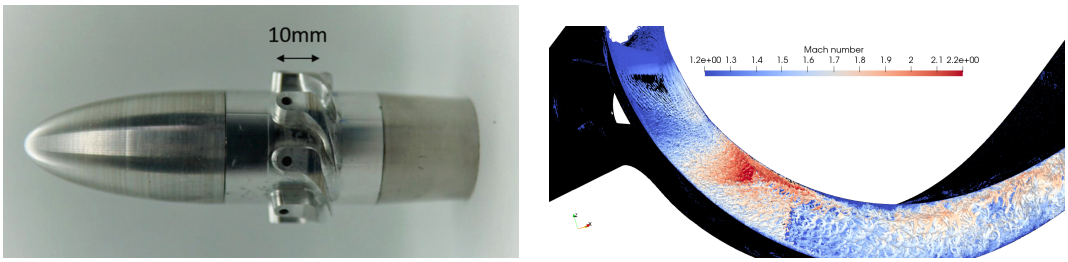


Figure 6: *a) Picture of the annular cascade[15] and b) Flow field visualization at the extrados of Q-criterion colored with the Mach number (WL-400M case).*

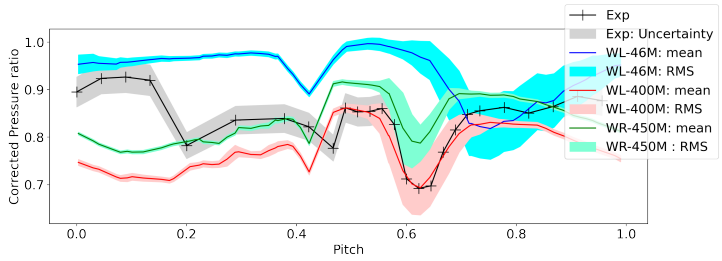


Figure 7: *Evolution of the total pressure ratio as a function of the pitch angle for three different meshes using an algebraic subgrid model (Wale model [12]). Comparison with experimental measurements[15].*

obtain an effective SGS model capable to provide reliable results for cases which were not encountered during the training phase. The *a posteriori* validation has been initiated by performing LES of a dense gas mixing layer at $M_c = 2.2$ using four grid sizes and three turbulent closure strategies: the ANN model was found to better predict growth rates for all grid sizes. Further results regarding the application of the ANN model in the context of an annular stator case are still being gathered and will be presented during the NICFD conference.

## 5 ACKNOWLEDMENTS

This work is supported by the JCJC ANR EDGES project, grant #ANR−17−CE06−0014−01 of the French Agence Nationale de la Recherche. Simulations have been carried out using HPC resources at CINES under the project grant #A0102A07564 . We also acknowledge PRACE for awarding us access to Joliot-Curie at GENCI@CEA, France. The authors would like to thank the CFD team at CERFACS for their support and for giving access to their solver AVBP. The authors would like to thank the PMCS2I team at Ecole Centrale de Lyon.

## REFERENCES

[1] D. Baumgärtner, J. J. Otter, and A. P. Wheeler. The effect of isentropic exponent on transonic turbine performance. Journal of Turbomachinery, 142(8), 2020.

[2] P. Cinnella and P. M. Congedo. Aerodynamic performance of transonic bethe-zel'dovich-thompson flows past an airfoil. AIAA journal, 43(2):370–378, 2005.

[3] O. Colin and M. Rudgyard. Development of high-order taylor–galerkin schemes for les. Journal of computational physics, 162(2):338–371, 2000.

[4] F. J. Durá Galiana, A. P. Wheeler, and J. Ong. A study of trailing-edge losses in organic rankine cycle turbines. Journal of Turbomachinery, 138(12):121003, 2016.

[5] F. D. Galiana, A. Wheeler, J. Ong, and C. de M Ventura. The effect of dense gas dynamics on loss in orc transonic turbines. In Journal of Physics: Conference Series, volume 821, page 012021. IOP Publishing, 2017.

[6] A. Giauque, C. Corre, and M. Menghetti. Direct numerical simulations of homogeneous isotropic turbulence in a dense gas. In Journal of Physics: Conference Series, volume 821, page 012017. IOP Publishing, 2017.

[7] A. Giauque, C. Corre, and A. Vadrot. Direct numerical simulations of forced homogeneous isotropic turbulence in a dense gas. Journal of Turbulence, 21(3):186–208, 2020.

[8] A. Giauque, A. Vadrot, P. Errante, and C. Corre. A priori analysis of subgrid-scale terms in compressible transcritical real gas flows. Physics of Fluids, 33(8):085126, 2021.

[9] G. Gori, M. Zocca, A. Guardone, O. Le Maitre, and P. M. Congedo. Bayesian inference of thermodynamic models from vapor flow experiments. Computers & Fluids, 205:104550, 2020.

[10] N. Gourdain, L. Gicquel, G. Staffelbach, O. Vermorel, F. Duchaine, J. Boussuge, and T. Poinsot. High performance parallel computing of flows in complex geometries: Ii. applications. Computational Science & Discovery, 2(1):015004, 2009.

[11] J.-C. Hoarau, P. Cinnella, and X. Gloerfelt. Large eddy simulations of strongly non-ideal compressible flows through a transonic cascade. Energies, 14(3):772, 2021.

[12] F. Nicoud and F. Ducros. Subgrid-scale stress modelling based on the square of the velocity gradient tensor. Flow, turbulence and Combustion, 62(3):183–200, 1999.

[13] F. Nicoud, H. B. Toda, O. Cabrit, S. Bose, and J. Lee. Using singular values to build a subgrid-scale model for large eddy simulations. Physics of fluids, 23(8):085106, 2011.

[14] P. Novello, G. Poëtte, D. Lugato, and P. Congedo. Explainable hyperparameters optimization using hilbert-schmidt independence criterion. 2021.

[15] J. J. Otter, D. Baumgärtner, and A. P. Wheeler. The development of a generic working fluid approach for the determination of transonic turbine loss. In International Seminar on Non-Ideal Compressible-Fluid Dynamics for Propulsion & Power, pages 123–131. Springer, 2020.

[16] N. Saura and T. Gomez. Subgrid stress tensor prediction in homogeneous isotropic turbulence using 3d-convolutional neural networks. Available at SSRN 4184202, 2022.

[17] G. Schnerr and P. Leidner. Nonclassical behavior of dense gases in axial cascades. Zeitschrift für angewandte Mathematik und Mechanik, 76:457–458, 1996.

[18] L. Sciacovelli, P. Cinnella, and X. Gloerfelt. Direct numerical simulations of supersonic turbulent channel flows of dense gases. Journal of Fluid Mechanics, 821:153–199, 2017.

[19] A. Vadrot. Numerical simulation and modeling of compressible turbulence in dense gas flows. PhD thesis, Université de Lyon, 2021.

[20] A. Vadrot, A. Giauque, and C. Corre. Analysis of turbulence characteristics in a temporal dense gas compressible mixing layer using direct numerical simulation. Journal of Fluid Mechanics, 893, 2020.

[21] A. Vadrot, A. Giauque, and C. Corre. Direct numerical simulations of temporal compressible mixing layers in a bethe–zel'dovich–thompson dense gas: influence of the convective mach number. Journal of Fluid Mechanics, 922, 2021.